

# Deep learning-based, computer-aided classifier developed with dermoscopic images shows comparable performance to 164 dermatologists in cutaneous disease diagnosis in the Chinese population

Shi-Qi Wang<sup>1</sup>, Xin-Yuan Zhang<sup>2</sup>, Jie Liu<sup>1</sup>, Cui Tao<sup>2</sup>, Chen-Yu Zhu<sup>1</sup>, Chang Shu<sup>1</sup>, Tao Xu<sup>3</sup>, Hong-Zhong Jin<sup>1</sup>

<sup>1</sup>Department of Dermatology, Peking Union Medical College Hospital, Chinese Academy of Medical Sciences and Peking Union Medical College, Beijing 100730, China;

<sup>2</sup>School of Biomedical Informatics, The University of Texas Health Science Center at Houston, Houston, TX 77030, USA;

<sup>3</sup>Department of Epidemiology and Statistics, School of Basic Medicine, Peking Union Medical College, Institute of Basic Medical Sciences, Chinese Academy of Medical Sciences, Beijing 100005, China.

## Abstract

**Background:** Diagnoses of Skin diseases are frequently delayed in China due to lack of dermatologists. A deep learning-based diagnosis supporting system can facilitate pre-screening patients to prioritize dermatologists' efforts. We aimed to evaluate the classification sensitivity and specificity of deep learning models to classify skin tumors and psoriasis for Chinese population with a modest number of dermoscopic images.

**Methods:** We developed a convolutional neural network (CNN) based on two datasets from a consecutive series of patients who underwent the dermoscopy in the clinic of the Department of Dermatology, Peking Union Medical College Hospital, between 2016 and 2018, prospectively. In order to evaluate the feasibility of the algorithm, we used two datasets. Dataset I consisted of 7192 dermoscopic images for a multi-class model to differentiate three most common skin tumors and other diseases. Dataset II consisted of 3115 dermoscopic images for a two-class model to classify psoriasis from other inflammatory diseases. We compared the performance of CNN with 164 dermatologists in a reader study with 130 dermoscopic images. The experts' consensus was used as the reference standard except for the cases of basal cell carcinoma (BCC), which were all confirmed by histopathology.

**Results:** The accuracies of multi-class and two-class models were  $81.49\% \pm 0.88\%$  and  $77.02\% \pm 1.81\%$ , respectively. In the reader study, for the multi-class tasks, the diagnosis sensitivity and specificity of 164 dermatologists were 0.770 and 0.962 for BCC, 0.807 and 0.897 for melanocytic nevus, 0.624 and 0.976 for seborrheic keratosis, 0.939 and 0.875 for the "others" group, respectively; the diagnosis sensitivity and specificity of multi-class CNN were 0.800 and 1.000 for BCC, 0.800 and 0.840 for melanocytic nevus, 0.850 and 0.940 for seborrheic keratosis, 0.750 and 0.940 for the "others" group, respectively. For the two-class tasks, the sensitivity and specificity of dermatologists and CNN for classifying psoriasis were 0.872 and 0.838, 1.000 and 0.605, respectively. Both the dermatologists and CNN achieved at least moderate consistency with the reference standard, and there was no significant difference in Kappa coefficients between them ( $P > 0.05$ ).

**Conclusions:** The performance of CNN developed with relatively modest number of dermoscopic images of skin tumors and psoriasis for Chinese population is comparable with 164 dermatologists. These two models could be used for screening in patients suspected with skin tumors and psoriasis respectively in primary care hospital.

**Keywords:** Artificial intelligence; Convolutional neural network; Skin tumor; Psoriasis; Dermoscopy

## Introduction

In China, the dermatologist to patient ratio is as low as 1:60,000. Also, most well-trained and experienced dermatologists are located in large cities, increasing scarcity of dermatologists in rural China.<sup>[1]</sup> Furthermore,

a considerable number of Chinese dermatologists and general physicians, especially those in the remote areas, due to limited clinical experience and learning opportunities, have low diagnostic accuracy for skin diseases. Therefore, a lot of patients with skin diseases could not see

Shi-Qi Wang and Xin-Yuan Zhang contributed equally to this work.

**Correspondence to:** Jie Liu, Department of Dermatology, Peking Union Medical College Hospital, No. 1 Shuaifuyuan, Dongcheng District, Beijing 100730, China  
E-Mail: liujie04672@pumch.cn; Cui Tao, School of Biomedical Informatics, The University of Texas Health Science Center at Houston, Houston, TX 77030, USA  
E-Mail: Cui.Tao@uth.tmc.edu

Copyright © 2020 The Chinese Medical Association, produced by Wolters Kluwer, Inc. under the CC-BY-NC-ND license. This is an open access article distributed under the terms of the Creative Commons Attribution-Non Commercial-No Derivatives License 4.0 (CCBY-NC-ND), where it is permissible to download and share the work provided it is properly cited. The work cannot be changed in any way or used commercially without permission from the journal.

Chinese Medical Journal 2020;133(17)

Received: 07-03-2020 Edited by: Li-Shao Guo

## Access this article online

Quick Response Code:



Website:  
www.cmj.org

DOI:  
10.1097/CM9.0000000000001023

a professional dermatologist in time or at all. So their diseases are often misdiagnosed or the treatments are delayed. There is an urgent need to improve the diagnosis accuracy of skin diseases in China.

As the most common malignant and benign skin tumors in the Chinese population, basal cell carcinoma (BCC), melanocytic nevus (MN), and seborrheic keratosis (SK) usually share similar clinical features, and are easily misdiagnosed. However, the preferred treatments for these tumors are quite different and a misdiagnosis could result in improper healthcare.<sup>[2-6]</sup> So it is of great significance to correctly diagnose BCC, MN, and SK.

As a major skin inflammatory disease, psoriasis has a prevalence of 2% to 4% worldwide.<sup>[7,8]</sup> It can lead to psychological problems for young people and decrease quality of life. For psoriasis diagnosis, it is crucial to rule out other conditions that result in delay of appropriate therapy, such as pityriasis rosea, lichen planus, eczema, and so on. Additionally, when scalp scaling occurs, it is necessary to rule out seborrheic dermatitis.<sup>[9]</sup> Therefore, the accurate diagnosis of psoriasis is very important.

The problem of classifying skin lesions has been a focus for the machine learning. Automated image classification can support dermatologists in their daily clinical practice and create faster and less expensive diagnosis assistance. Deep learning, a branch of machine learning, attempts to extract high-level information from data.<sup>[10]</sup> The convolutional neural network (CNN) can perform feature extraction implicitly and learn sophisticated representations of the image.<sup>[10,11]</sup> One advantage of CNN is that it is not necessary to pre-process the images for classification, which is a key step of traditional machine learning.<sup>[12]</sup> CNN systems become more accurate as the data volume increases. However, one of the largest barrier to using deep learning effectively in the medical field is the lack of datasets.<sup>[13]</sup>

Our current study was designed to investigate whether a CNN-based artificial intelligence (AI) model can be used to develop an efficient skin tumor or psoriasis classification system with a modest number of dermoscopic images. We chose dermoscopic images rather than clinical pictures for the following reasons: (1) most skin diseases have specific characteristics under dermoscopy, which is useful for improving the diagnostic accuracy of cutaneous diseases<sup>[14-17]</sup>; and (2) the dermoscopic image is a magnified image of the lesion with a simple background, few interference factors, and obvious structures, suitable for input into the computer.

In order to evaluate the feasibility of the algorithm, we used two datasets. First, BCC, MN, and SK were selected as the three main target diseases in dataset I to build a multiclass model; psoriasis, acne vulgaris, dermatofibroma, and cutaneous haemangioma, which are common types of tumors or skin inflammatory diseases, were collectively called “others.” The “others” group was used to represent the images that did not belong to the three target categories to increase the model’s screening specificity. Then, we collected dataset II to include psoriasis and other

inflammatory cutaneous diseases for developing a two-class model; other inflammatory diseases included seborrheic dermatitis, eczema, lichen planus, and pityriasis rosea. Furthermore, the two models’ performances were compared with the diagnoses of 164 board-certified Chinese dermatologists. This tool could potentially be used as a pre-screening tool to assist general physicians to make recommendations or for dermatologists to prioritize their efforts and lay the foundation for precision medicine and remote consultation.

## Methods

### Ethical approval

All procedures involving humans were carried out in accordance with the ethical standards of the 2013 *Declaration of Helsinki* and were approved by the Medical Ethics Committee of Peking Union Medical College Hospital. Informed consent was obtained from all participants.

### Datasets

All images were consecutively collected from the clinic of the Department of Dermatology, Peking Union Medical College Hospital, between 2016 and 2018 prospectively. The patients were all Asian with the type IV of Fitzpatrick skin types. The images were all obtained by MoleMax HD 1.0 dermoscope (Derma Medical Systems, Vienna, Austria). All BCCs were confirmed by histopathology. The diagnosis of other disease was made according to the criteria in the expert consensus or guidelines published<sup>[18-21]</sup> and the annotation process is seen in Figure 1. The annotation process in details is as follows: (1) two experts who were with more than 5 years of work experience blinded with each other provided a consistent interpretation of the dermoscopic image combining the clinical image and medical histories; (2) If there is a disagreement, a third expert would be the tie breaker; (3) If the three experts still could not get an agreement, the confusing cases would be excluded. The images which have poor focus, include multiple lesions or show interference factors such as clothing

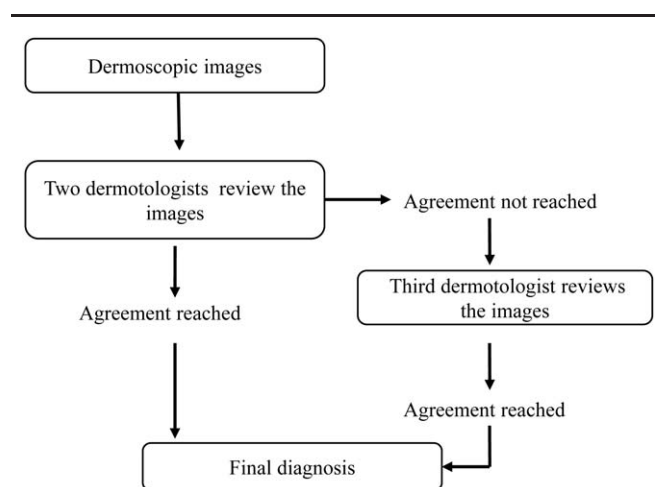


Figure 1: The annotation process of dermoscopic images.

**Table 1: Characteristics of dataset I and II for the multi- and two-class model respectively.\***

Characteristics	Development set		Test set of the reader study	
	Images	Patients	Images	Patients
Dataset I				
Years	2016–2018	2016–2018	2018	2018
Number included in study ( <i>n</i> )	7192	1484	70	70
Mean age (years), mean ± SD (range)	–	47 ± 19 (4–95)	–	49 ± 19 (12–95)
Female, <i>n</i> (%)	–	881 (59.36)	–	39 (55.71)
Basal cell carcinoma, <i>n</i> (%)	368 (5.12)	82 (5.53)	10 (14.29)	10 (14.29)
Melanocytic nevus, <i>n</i> (%)	1872 (26.03)	464 (31.27)	20 (28.57)	20 (28.57)
Seborrheic keratosis, <i>n</i> (%)	1887 (26.24)	448 (30.19)	20 (28.57)	20 (28.57)
Others, <i>n</i> (%)	3065 (42.49)	490 (33.02)	20 (28.57)	20 (28.57)
Dataset II				
Years	2016–2018	2016–2018	2018	2018
Number included in study ( <i>n</i> )	3115	501	60	60
Mean age (years), mean ± SD (range)	–	40 ± 16 (6–87)	–	43 ± 19 (14–89)
Female, <i>n</i> (%)	–	249 (49.70)	–	33 (55.00)
Psoriasis, <i>n</i> (%)	2101 (67.45)	326 (65.07)	22 (36.67)	22 (36.67)
Other inflammatory diseases, <i>n</i> (%)	1014 (32.55)	175 (34.93)	38 (63.33)	38 (63.33)

The CNN model trained by dataset I, which involved four categories, was named as multi-class model; similarly, the CNN model trained by dataset II, which involved two categories, was named as two-class model. CNN: Convolutional neural network; SD: Standard deviation.

fiber, written notes or hair (except for scalp psoriasis and scalp seborrheic dermatitis), and the lesions located in the nail or mucosa were also excluded. The datasets used and patient demographic characteristics are in Table 1. The category of SK did not include solar lentigo and lichen planus-like keratosis. In most cases, multiple dermoscopic images of a single lesion, including different angles or close-ups, were photographed. Some example pictures of dataset I and dataset II are shown in Figure 2.

### CNN and deep learning algorithm

Both datasets were divided into training, validation, and testing sets in an 8:1:1 ratio.<sup>[22]</sup> Ten-fold cross-validation was performed to verify the robustness of the model. The validation set was separated from the training set to avoid overfitting.<sup>[23]</sup> The images were divided by patient to prevent images of the same patient being used in both training/validating and testing. In order to verify the methodology published by the Stanford University<sup>[24]</sup> and to test the applicability for the cases of Chinese hospitals, we developed our algorithm based on the pre-trained CNN parameters from GoogLeNet Inception v3 using the ImageNet dataset.<sup>[25]</sup> ImageNet contains over 1.28 million images for over 1000 normal life objects.<sup>[22]</sup> We re-trained the final layer with our images as input, using “ReLU” as our activation function and “Gradient Descent Optimizer” as our optimizer with a learning rate of “0.01.” “Cross entropy mean” was used to minimize the loss function.

The format of the input vectors in the input layer is a numeric matrix, where each element in the matrix is one pixel in the input image. For example, if an image has 864 pixels, multiplied by red, green, and blue layers, the number of elements in the matrix would be 2592. If there are 1000 input images, the input matrix will have the

dimension of  $2592 \times 1000$ . A feature map was obtained by applying a linear filter and a non-linear function to the input matrix. For example, the hidden layer  $A^k$ , where  $k$  is the  $k^{\text{th}}$  feature map. The filters consisted of weight  $W^k$  and bias  $b_k$ . The feature map  $A^k$  was calculated using Formula 1. Then, the feature map calculated from extraction was classified. Each hidden layer was composed of multiple feature maps. There were a total of 28 layers in our model, including input and output layers. The simplified framework of our CNN model structure is shown in Figure 3. More detailed code regarding the retraining process publicly released on Github can be found at: [https://github.com/tensorflow/hub/blob/master/examples/image\\_retraining/retrain.py](https://github.com/tensorflow/hub/blob/master/examples/image_retraining/retrain.py).

$$A_{ij}^k = \tanh((W^k \cdot x)_{ij} + b_k) \quad (1)$$

### Visualization of internal features

T-distributed Stochastic Neighbor Embedding (t-SNE) plot, a method for visualizing high-dimensional data, was employed to show the internal features learned by the CNN.<sup>[24]</sup> Each point represents a skin lesion image projected from the output of the CNN’s last hidden layer into two dimensions.<sup>[24]</sup>

### Evaluation

#### Performance of CNN for the multi and two-class models

Each test image was given a probability for each of the two or four disease categories, summing to 1. The highest probability was regarded as the classification category. We calculated the accuracy, specificity, sensitivity, and area under the receiver operating characteristic (ROC) curve

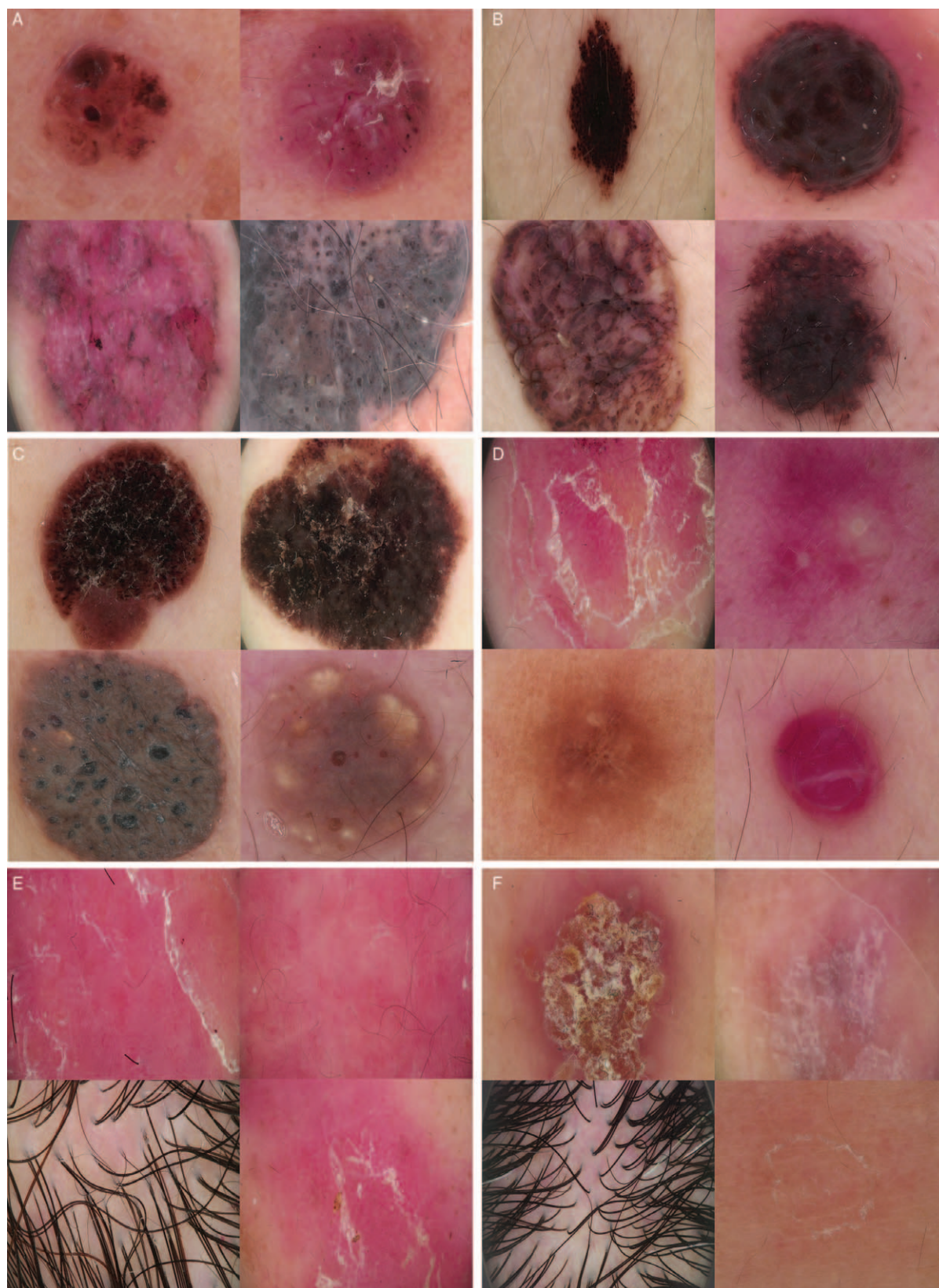


**Figure 2:** Example dermoscopic images: basal cell carcinoma (A), melanocytic nevus (B), seborrheic keratosis (C), “others” (D) including psoriasis (upper left), acne vulgaris (upper right), dermatofibroma (bottom left), and cutaneous haemangioma (bottom right). These images highlight the difficulty of classification: Psoriasis (E), other inflammatory diseases (F) involving eczema (upper left), lichen planus (upper right), seborrheic dermatitis (bottom left), and pityriasis rosea (bottom right).

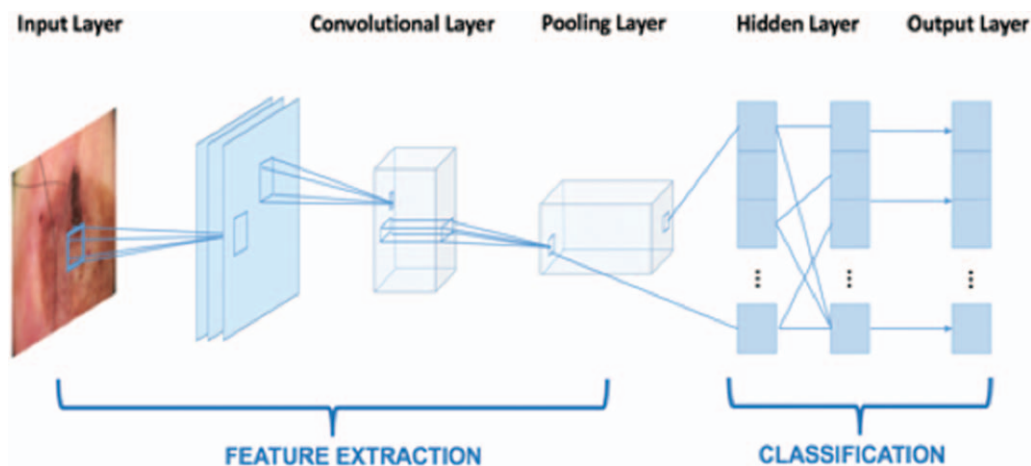


**Figure 3:** The simplified framework of convolutional neural network.

(AUC) for each category. The confusion matrix<sup>[26]</sup> was also employed to evaluate the multiclass models. It is a specific table layout that visualizes the performance of the algorithm. The abscissa represents the true label, the ordinate represents the prediction label, and the number in each column shows the instances in a predicted class.

### Comparison between CNN and dermatologists

The classification sensitivity and specificity of our CNN-based classifier was compared against Chinese board-certified dermatologists in a reader study. In the experiment, 164 dermatologists who finished more than 10 h of systematic dermoscopic knowledge training and our algorithm classified the same 130 images; the images were selected on a patient-by-patient basis and there was no overlap of patients between the 130 images and the training, validation, and testing sets.

Each dermatologist was given a questionnaire that comprised two parts of images (70 images for the multiclass model and 60 images for the two-class model) through screen sharing. All participating dermatologists were required to answer this questionnaire in the same room at the same time. The corresponding clinical pictures were provided in a small size and no other information was offered. We should note that the clinical picture was provided to dermatologists but not to the AI. The reason is that the dermatologists will definitely look at the clinical picture firstly in the real clinical practice, they rarely directly gave a diagnosis according to the dermoscopic picture only. On the other hand, according to our experience, training AI with clinical pictures and dermoscopic images will reduce the accuracy. Therefore, when training and testing AI, solely dermoscopic images were provided. The gold standard was created by biopsy (BCC) and expert consensus (all others).

### Statistical analysis

In the reader study, sensitivity, specialty, and their 95% confidence interval (CI) were calculated. Kappa coefficients were used to assess the consistency between

dermatologists (or CNN) and the reference standard on the classification of each disease. Kappa coefficient  $>0.75$  indicates good consistency, 0.40 to 0.75 indicates moderate consistency, and  $<0.40$  indicates poor consistency. Adjusted Z-tests were used to assess differences in Kappa coefficients between dermatologists and CNN. Results were considered statistically significant at the  $P < 0.05$  level. All analyses were carried out using SAS 9.4 (SAS Institute Inc., Cary, NC, USA).

## Results

### Performance of CNN for the multiclass model

The average accuracy  $\pm$  standard deviation was  $81.49\% \pm 0.88\%$ . The fluctuation of the accuracy of classification was only  $\pm 0.88\%$ , demonstrating robustness of the CNN. The diagnosis sensitivity and specificity were  $0.825 \pm 0.060$  and  $0.960 \pm 0.007$  for BCC,  $0.789 \pm 0.015$  and  $0.923 \pm 0.008$  for MN,  $0.749 \pm 0.029$  and  $0.920 \pm 0.008$  for SK,  $0.869 \pm 0.017$  and  $0.936 \pm 0.010$  for the “others” group. The AUC scores of diagnosing BCC, MN, SK, and “others” were  $0.972 \pm 0.011$ ,  $0.952 \pm 0.014$ ,  $0.933 \pm 0.014$ , and  $0.965 \pm 0.005$ , respectively. The ROC graphs and the corresponding confusion matrix for each category from one experiment are shown in Figure 4A–4D and Table 2.

### Performance of CNN for the two-class model

The average accuracy of the “psoriasis *vs.* other inflammatory diseases” group was  $77.02\% \pm 1.81\%$ . The two-class model achieved  $0.797 \pm 0.040$  sensitivity and  $0.719 \pm 0.078$  specificity for psoriasis. The ROC graphs for each category from one experiment are shown in Figure 4E and 4F. And the average AUC for this binary classification model is  $0.840 \pm 0.022$ .

### Comparison between CNN and dermatologists

The general information of the 164 board-certified dermatologists is shown in Table 3. As Table 4 shows,

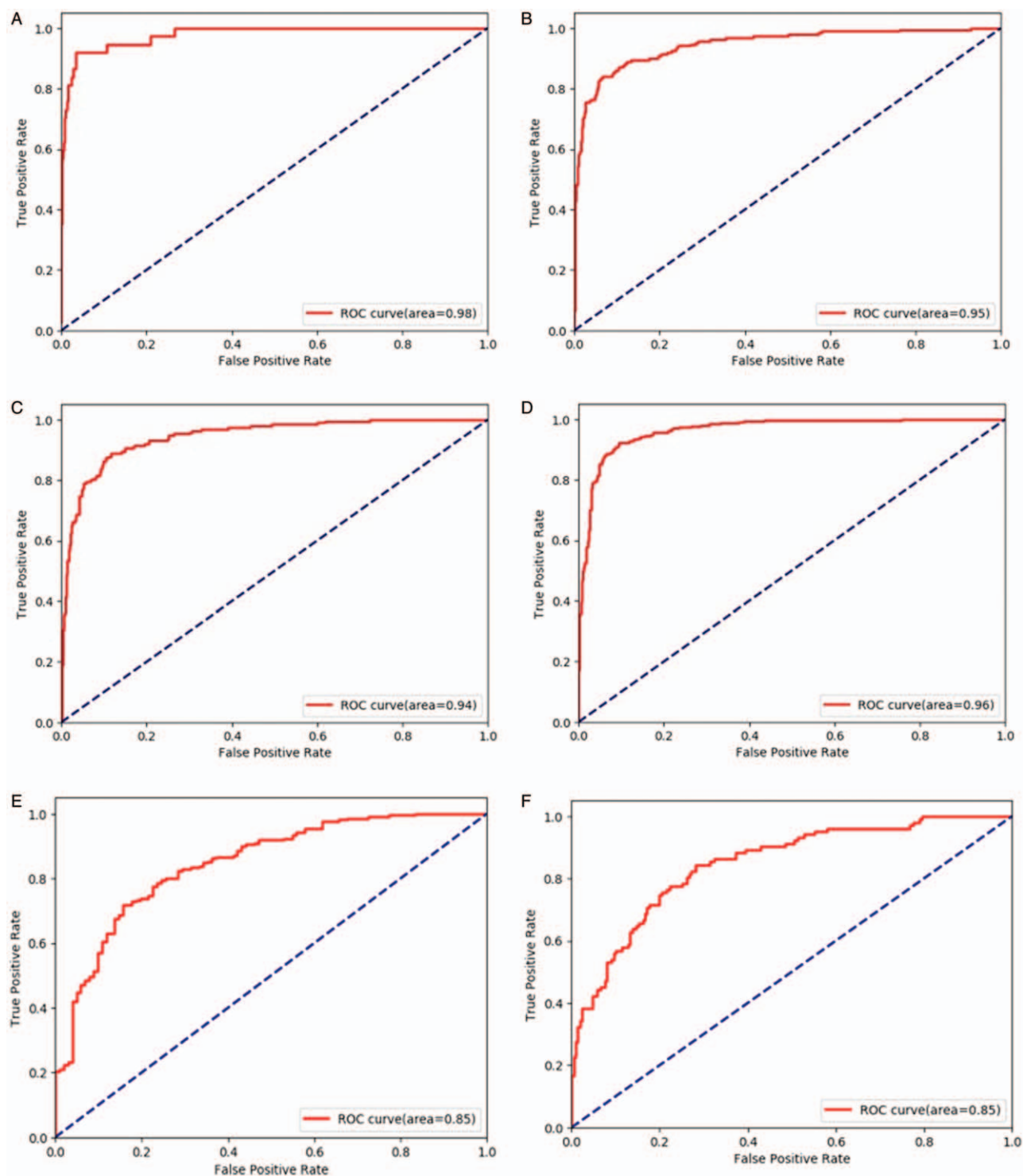


**Figure 4:** Receiver operating characteristic (ROC) graphs for basal cell carcinoma (A), melanocytic nevus (B), seborrheic keratosis (C), and other groups (D) for one test of the ten-fold cross-validation, which comes from the same test as Table 4. ROC graphs for psoriasis (E) vs. other inflammation conditions (F) for one test of the ten-fold cross-validation.

in the multi-class tasks, the diagnosis sensitivity and specificity of 164 dermatologists were 0.770 (95% CI 0.415–0.952) and 0.962 (95% CI 0.868–0.992) for BCC, 0.807 (95% CI 0.565–0.938) and 0.897 (95% CI 0.770–0.961) for MN, 0.624 (95% CI 0.386–0.818) and 0.976 (95% CI 0.874–0.998) for SK, 0.939 (95% CI 0.716–0.995) and 0.875 (95% CI 0.744–0.947) for the “others” group, respectively; the diagnosis sensitivity and specificity

of multi-class CNN were 0.800 (95% CI 0.442–0.965) and 1.000 (95% CI 0.925–1.000) for BCC, 0.800 (95% CI 0.557–0.934) and 0.840 (95% CI 0.703–0.924) for MN, 0.850 (95% CI 0.611–0.960) and 0.940 (95% CI 0.825–0.984) for SK, 0.750 (95% CI 0.506–0.904) and 0.940 (95% CI 0.825–0.984) for the “others” group, respectively. In the two-class tasks, the sensitivity and specificity of dermatologists and CNN for classifying psoriasis were

**Table 2: Confusion matrix of CNN in one test of ten-fold cross-validation.**

Predicted label	True label			
	BCC	MN	SK	Others
BCC	30 <sup>*</sup>	4 <sup>‡</sup>	6 <sup>‡</sup>	6 <sup>‡</sup>
MN	3 <sup>†</sup>	154 <sup>*</sup>	14 <sup>†</sup>	14 <sup>‡</sup>
SK	3 <sup>†</sup>	16 <sup>†</sup>	152 <sup>*</sup>	12 <sup>‡</sup>
Others	1 <sup>‡</sup>	13 <sup>†</sup>	17 <sup>†</sup>	275 <sup>*</sup>
Total	37	187	189	307
Accuracy (%)	81.08	82.35	80.42	89.58

The abscissa of the confusion matrix represents the true label, the ordinate represents the prediction label, and the number in each column shows the instances in a predicted class. The diagonal line represents the correct numbers of cases in which each group of diseases was diagnosed correctly. Based on the confusion matrix, all categories reached 80% classification accuracy, and the probability of each disease being misdiagnosed as one of the other three categories was less than 12%. Percentage within each column: <sup>\*</sup>Greater than 50%, <sup>†</sup>Greater than 5% but less than 12%, <sup>‡</sup>less than 5%. BCC: Basal cell carcinoma; CNN: Convolutional neural network; MN: Melanocytic nevus; SK: Seborrheic keratosis.

**Table 3: Demographics of 164 board-certified Chinese dermatologists.**

Characteristics	Results, <i>n</i> (%)
Age (years)	
<30	39 (23.8)
31–40	70 (42.7)
41–50	40 (24.4)
>50	15 (9.1)
Sex	
Male	41 (25.0)
Female	123 (75.0)
Experience of dermatology (years)	
1.0–3.0	38 (24.8)
3.1–5.0	24 (15.7)
5.1–10.0	33 (21.6)
10.1–20.0	32 (20.9)
>20.0	26 (17.0)

**Table 4: The classification sensitivity, specificity, and Kappa coefficient compared with reference standard of 164 board-certified dermatologists and the CNN.**

Disease category	Dermatologists	CNN	<i>P</i> value
<b>Multi-class model</b>			
Basal cell carcinoma			
Sensitivity (95% CI)	0.770 (0.415–0.952)	0.800 (0.442–0.965)	–
Specificity (95% CI)	0.962 (0.868–0.992)	1.000 (0.925–1.000)	–
Kappa coefficient (95% CI) <sup>*</sup>	0.732 (0.500–0.964)	0.873 (0.700–1.000)	0.459
Melanocytic nevus			
Sensitivity (95% CI)	0.807 (0.565–0.938)	0.800 (0.557–0.934)	–
Specificity (95% CI)	0.897 (0.770–0.961)	0.840 (0.703–0.924)	–
Kappa coefficient <sup>*</sup>	0.690 (0.503–0.877)	0.604 (0.404–0.804)	0.537
Seborrheic keratosis			
Sensitivity (95% CI)	0.624 (0.386–0.818)	0.850 (0.611–0.960)	–
Specificity (95% CI)	0.976 (0.874–0.998)	0.940 (0.825–0.984)	–
Kappa coefficient (95% CI) <sup>*</sup>	0.662 (0.461–0.864)	0.790 (0.630–0.950)	0.331
Others			
Sensitivity (95% CI)	0.939 (0.716–0.995)	0.750 (0.506–0.904)	–
Specificity (95% CI)	0.875 (0.744–0.947)	0.940 (0.825–0.984)	–
Kappa coefficient (95% CI) <sup>*</sup>	0.757 (0.595–0.920)	0.711 (0.525–0.897)	0.714
<b>Two-class model</b>			
Psoriasis			
Sensitivity (95% CI)	0.872 (0.650–0.968)	1.000 (0.815–1.000)	–
Specificity (95% CI)	0.838 (0.677–0.932)	0.605 (0.435–0.755)	–
Kappa coefficient (95% CI) <sup>*</sup>	0.688 (0.502–0.875)	0.529 (0.502–0.875)	0.232

CI: Confidence interval; CNN: Convolutional neural network. <sup>\*</sup> Compared with reference standard.

0.872 (95% CI 0.650–0.968) and 0.838 (95% CI 0.677–0.932), 1.000 (95% CI 0.815–1.000) and 0.605 (95% CI 0.435–0.755), respectively. Both the dermatologists and CNN achieved at least moderate evaluation consistency with the reference standard, and there was no significant difference in Kappa coefficients between them (*P* > 0.05).

**Visualization of internal features**

Each point in the t-SNE plot represents a dermoscopic image. Similar images are more likely to be clustered

together. We used the test set from one experiment for the multiclass model in Figure 5A. All images in the experiment for the multiclass model are plotted in Figure 5B.

**Discussion**

In recent years, several studies have reported the application of deep learning for the classification of skin diseases, especially skin tumors.<sup>[27-37]</sup> Most of them used the pre-trained ResNet50 CNN network,<sup>[33-37]</sup> using images from the International Skin Imaging Collaboration. To verify the

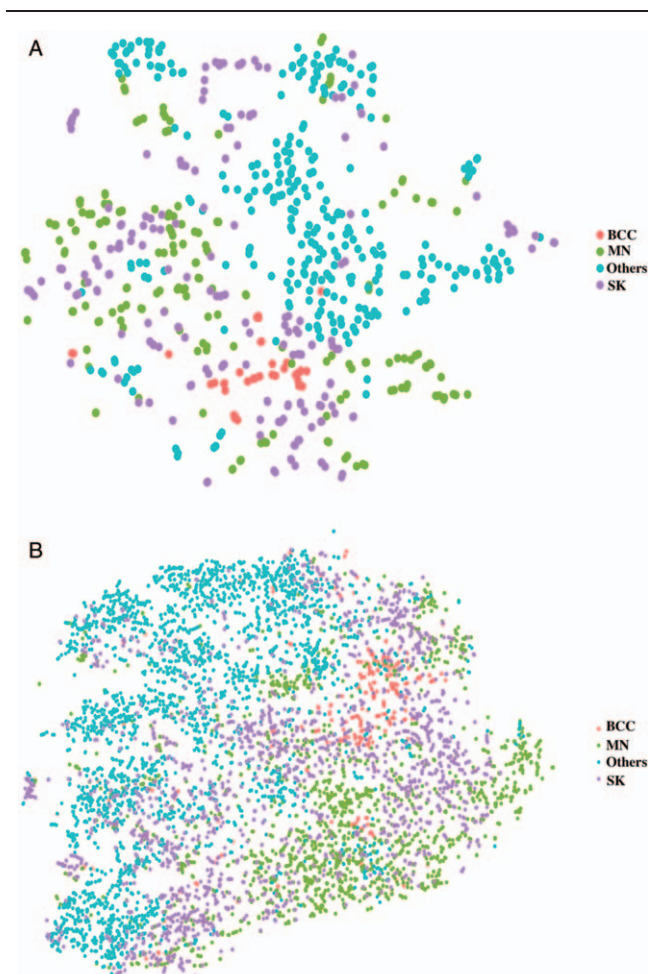


**Figure 5:** The Stochastic Neighbor Embedding (t-SNE) plot of the multi-class model. (A) The red cluster below represents the BCC cluster. The blue cluster has several subgroups, corresponding to multiple disease types in the “others” group. The patterns for MN and SK classes are not revealed. (B) When using all the images, the pattern of MN is seen to distribute mostly in the bottom right corner. The clusters for SK are split crossed. The pattern for the “others” and BCC groups is similar to Figure (A). BCC: Basal cell carcinoma; CNN: Convolutional neural network; MN: Melanocytic nevus; SK: Seborrheic keratosis.

consistency of results published by the Stanford University<sup>[24]</sup> for Chinese hospital use cases, we developed the algorithm based on the pre-trained GoogLeNet Inception v3 CNN network for our own dataset. As for the disease spectrum, they were mostly focused on distinguishing melanoma, nevi or skin cancer images. Images of inflammatory skin conditions, including psoriasis and acne vulgaris, were innovatively added to the multiclass training dataset for skin tumor classification in this study to verify the CNN’s ability to learn dermoscopic features of inflammatory skin diseases, and to determine whether CNN can distinguish skin tumors from inflammatory skin conditions. This is the first study, to the best of our knowledge, focusing on using deep-learning-based approach to automatically classify dermoscopic images for most common skin diseases in Chinese population. The study includes the most common skin tumors and inflammatory diseases in China. Melanoma is excluded from the classification list because the incidence of malignant melanoma in the Chinese population is relatively low (less than 1/100,000<sup>[38]</sup>) and the number of pictures is limited. From 2014 to 2018, we collected about 130,000 dermoscopic images that include about 14,000

cases in total. However, it contains only 25 cases of malignant melanoma (188 dermoscopic images); and 89/188 images are further excluded because they are located in the nail or with notes. Moreover, the most common type is the acral malignant melanoma (41.8%),<sup>[38]</sup> and the superficial type is relatively rare. It is relatively easy to diagnosis acral malignant melanoma as the associated features are usually easy to be distinguished from other tumors. Therefore, the skin tumors in this study do not contain malignant melanoma, but focus on three most common skin tumors (BCC, melanocytic nevus, and SK).

In previous studies, Esteva *et al*<sup>[24]</sup> used 129,450 images and demonstrated that a CNN could achieve dermatologist-level classification of skin cancer, including keratinocytic and melanocytic tumors. In the study of Fujisawa *et al*,<sup>[22]</sup> CNNs were trained on approximately 5% (4867 images) that number of images; for 14 skin tumors, the overall classification accuracy of the CNN was 76.5%, which was a statistically higher accuracy than the board-certified dermatologists. Similar to Fujisawa’s study, satisfactory overall classification accuracies (81.49% and 77.02%) were achieved using modest datasets (7192 and 3115 images) in our study, which showed that, as long as the images were correctly labeled, a well-performed CNN classifier can be developed using a much smaller training dataset.

Our previous study, which tested over 1000 dermoscopic images for the model of four classes, had an average accuracy of  $87.25\% \pm 2.24\%$ .<sup>[28]</sup> The robustness of our algorithm improved; however, the accuracy decreased from 87.25% to 81.49%. A possible reason could be the images in the “others” group, which included inflammatory skin conditions. It might be difficult for CNN to generate key features for classification of many different skin diseases within the same category. The results of the “Performance of CNN for the multiclass model” showed that the SK group had the worst performance, while the accuracy of SK in the reader study was the best. It demonstrated that the differences in the level of difficulty inherent to images of the test set will directly impact the diagnostic performance of the algorithms.

To serve as a reference comparator to the automated algorithm, it is of the utmost importance to include a large group of dermatologists.<sup>[39]</sup> This study compared CNN diagnostic performance to 164 Chinese dermatologists with more than 10 h of systematic dermoscopy training. To the best of our knowledge, this was the largest group of dermatologists involved for such studies. In Fujisawa’s study, the accuracy of 13 board-certified dermatologists and nine dermatology trainees was compared to the accuracy of their CNN.<sup>[22]</sup> Han *et al*<sup>[29]</sup> compared the accuracy of a computer classifier to 16 dermatologist board members. The publication of Haenssle *et al*<sup>[27]</sup> included 58 dermatologists in the comparison with CNN’s diagnostic performance. Our previous study included 95 experienced dermatologists who had received dermoscopy training in the differential diagnosis of pigmented nevus and SK. We concluded that performance of CNN automatic classification model is similar to that of experienced dermatologists in the two classification of pigmented nevus and SK.<sup>[40]</sup> And recently, it



has been reported that deep learning outperformed 112 dermatologists or 136 of 157 dermatologists in a dermoscopic melanoma image classification task or multiclass skin cancer image classification.<sup>[33,36]</sup> This demonstrates that our models are as accurate as large-scale trained dermatologists, and may potentially be used as a pre-screening tool to assist general physicians to make recommendations or for dermatologists to prioritize their efforts, especially since a considerable number of Chinese dermatologists do not have systematic training in dermoscopy.

Furthermore, we developed a two-class model for psoriasis and other inflammatory diseases as a pilot test and achieved an average accuracy of 77.02%. The prevalence of psoriasis is about 0.59% in China<sup>[41]</sup> and the involved population reached up to 8.26 million. It is a cosmetically debilitating and chronic disease which occurs both in developing and developed countries. In many hospitals in China, misdiagnosis and missed diagnosis of psoriasis occur often. To the best of our knowledge, there is currently no differential diagnosis model for dermoscopic images of psoriasis and other inflammatory diseases for Chinese population. This model achieved 100% sensitivity during the competition of 164 dermatologists *vs.* computer algorithm which has the potential to help dermatologists improve the early diagnosis and treatment of psoriasis significantly. It shows that our model prefers to classify the image under the category of “psoriasis,” and all the real psoriasis images are classified correctly. We might need to adjust the weights of two classes during the training process. Since the size of our second testing set is relatively small, 22 images for psoriasis group and 38 images for the other group, the accuracy, sensitivity, and specificity results from ten-fold cross validation are more valued. And these results also indicate that our model was not over-fitting. Unfortunately, other inflammatory disease groups here included only seborrheic dermatitis, eczema, lichen planus, and pityriasis rosea. Larger datasets including data on more psoriasis-related diseases are needed to develop a more efficient classification model for psoriasis in the future.

There are several limitations to our study. First, our dataset was created using only the database of the dermatology department of the Peking Union Medical College Hospital; due to the lack of diversity, it is possible that the sensitivity and specificity will be different when a different dataset is used. Second, although CNN achieved equal accuracy to the dermatologists in our study, this classification was based on the information obtained from only dermoscopic images (for CNN) or dermoscopic and clinical images (for dermatologists). If additional information, such as location, tactility, clinical course, subjective symptoms, age, and sex of the patients, were provided, the classification accuracy may be different.<sup>[42]</sup> Further studies are needed to clarify this hypothesis. Third, the dataset covered only 11 diseases and lacked the full spectrum of skin lesions encountered in clinical practice. To overcome this issue, future research can focus on ensuring the diagnostic sensitivity and specificity of the CNN model for each disease while increasing the categories of diseases.

In conclusion, we used a CNN trained with modest numbers of dermoscopic images from the Chinese population to develop two efficient skin disease classifiers.

Based on a single dermoscopic image, the performance of this CNN was comparable to 164 board-certified dermatologists with more than 10 h of dermoscopy systematic training in the classification of skin tumors and psoriasis. Next, we will apply this system to a professional medical network platform open to dermatologists in China (<https://ai.dxy.cn>) to find more ways to improve the models' classification performance.

### Acknowledgements

The authors would like to thank Yangzhige He of the Department of Medical Research Center, Peking Union Medical College Hospital, Chinese Academy of Medical Science & Peking Union Medical College, for her suggestions about the statistical analysis.

### Funding

This work was supported by grants from the Beijing Natural Science Foundation (No. 7182127), the National Natural Science Foundation of China (No. 61871011), the National Key Research and Development Program of China (No. 2016YFC0901500), the Non-profit Central Research Institute Fund of Chinese Academy of Medical Sciences (No. 2019XK320024), and the CAMS Innovation Fund for Medical Sciences (No. 2017-I2M-3-020).

### Conflicts of interest

None.

### References

- Zhao S, Xie B, Li Y, Zhao X, Kuang Y, Su J, *et al.* Smart identification of psoriasis by images using convolutional neural networks: a case study in China. *J Eur Acad Dermatol Venereol* 2020;34:518–524. doi: 10.1111/jdv.15965.
- Bobadilla F, Wortsman X, Munoz C, Segovia L, Espinoza M, Jemec GB. Pre-surgical high resolution ultrasound of facial basal cell carcinoma: correlation with histology. *Cancer Imaging* 2008;8:163–172. doi: 10.1102/1470-7330.2008.0026.
- Christenson LJ, Borrowman TA, Vachon CM, Tollefson MM, Otley CC, Weaver AL, *et al.* Incidence of basal cell and squamous cell carcinomas in a population younger than 40 years. *JAMA* 2005;294:681–690. doi: 10.1001/jama.294.6.681.
- Hauschild A, Egberts F, Garbe C, Bauer J, Grabbe S, Hamm H, *et al.* Melanocytic nevi. *J Dtsch Dermatol Ges* 2011;9:723–734. doi: 10.1111/j.1610-0387.2011.07741.x.
- Minagawa A. Dermoscopy-pathology relationship in seborrheic keratosis. *J Dermatol* 2017;44:518–524. doi: 10.1111/1346-8138.13657.
- Jackson JM, Alexis A, Berman B, Berson DS, Taylor S, Weiss JS. Current understanding of seborrheic keratosis: prevalence, etiology, clinical presentation, diagnosis, and management. *J Drugs Dermatol* 2015;14:1119–1125.
- Armstrong AW. Psoriasis. *JAMA Dermatol* 2017;153:956. doi: 10.1001/jamadermatol.2017.2103.
- Daniyal M, Akram M, Zainab R, Munir N, Shah SMA, Liu B, *et al.* Progress and prospects in the management of Psoriasis and developments in Phyto-therapeutic modalities. *Dermatol Ther* 2019;32:e12866. doi: 10.1111/dth.12866.
- Napolitano M, Caso F, Scarpa R, Megna M, Patri A, Balato N, *et al.* Psoriatic arthritis and psoriasis: differential diagnosis. *Clin Rheumatol* 2016;35:1893–1901. doi: 10.1007/s10067-016-3295-9.
- LeCun Y, Bengio Y, Hinton G. Deep learning. *Nature* 2015;521:436–444. doi: 10.1038/nature14539.
- Kumar A, Kim J, Lyndon D, Fulham M, Feng D. An ensemble of fine-tuned convolutional neural networks for medical image classification.

- IEEE J Biomed Health Inform 2017;21:31–40. doi: 10.1109/JBHI.2016.2635663.
12. Mai SM, Sheha MA, Sharawy A. Automatic detection of melanoma skin cancer using texture analysis. *Int J Comput Appl* 2012;42:22–26. doi: 10.5120/5817-8129.
  13. Han SS, Park GH, Lim W, Kim MS, Na JI, Park I, *et al.* Deep neural networks show an equivalent and often superior performance to dermatologists in onychomycosis diagnosis: automatic construction of onychomycosis datasets by region-based convolutional deep neural network. *PLoS One* 2018;13:e0191493. doi: 10.1371/journal.pone.0191493.
  14. Vestergaard ME, Macaskill P, Holt PE, Menzies SW. Dermoscopy compared with naked eye examination for the diagnosis of primary melanoma: a meta-analysis of studies performed in a clinical setting. *Br J Dermatol* 2008;159:669–676. doi: 10.1111/j.1365-2133.2008.08713.x.
  15. Rosendahl C, Tschandl P, Cameron A, Kittler H. Diagnostic accuracy of dermatoscopy for melanocytic and nonmelanocytic pigmented lesions. *J Am Acad Dermatol* 2011;64:1068–1073. doi: 10.1016/j.jaad.2010.03.039.
  16. Braun RP, Ludwig S, Marghoob AA. Differential diagnosis of seborrheic keratosis: clinical and dermoscopic features. *J Drugs Dermatol* 2017;16:835–842.
  17. Errichetti E, Stinco G. Dermoscopy in general dermatology: a practical overview. *Dermatol Ther (Heidelb)* 2016;6:471–507. doi: 10.1007/s13555-016-0141-6.
  18. Skin Imaging Group, Combination of Traditional and Western Medicine Dermatology; Skin Imaging Group, China International Exchange and Promotion Association for Medical and Healthcare; Skin Imaging Group, Chinese Society of Dermatology, Subcommittee on Dermatologic Surgery, China Dermatologist Association; Skin Imaging Equipment Group, Committee on Skin Disease and Cosmetic Dermatology, China Association of Medical Equipment. Dermoscopic characteristics of basal cell carcinoma: a Chinese expert consensus statement (2019) (in Chinese). *Chin J Dermatol* 2019;52:371–377. doi: 10.3760/cma.j.issn.0412-4030.2019.06.001.
  19. National Clinical Research Center for Skin and Immune Diseases; Huaxia Shin Image and Artificial Intelligence Cooperation, China International Exchange and Promotion Association for Medical and Healthcare; Skin Imaging Group, Dermatology Branch of China International Exchange and Promotion Association for Medical and Healthcare; Skin Imaging Group, Combination of Traditional and Western Medicine Dermatology; Subcommittee on Dermatologic Surgery, China Dermatologist Association; Skin Imaging Group (Preparing), Chinese Society of Dermatology, *et al.* Dermoscopic features of solar lentigo, seborrheic keratosis and lichen planus-like keratosis: an expert consensus statement (in Chinese). *Chin J Dermatol* 2019;52:878–883. doi: 10.35541/cjd.20190480.20.
  20. Qiao JJ, Zou XB, Dong HT, Xin LL. The diagnosis of dermoscopy in pigmented nevus (in Chinese). *Chin J Leprosy Skin Dis* 2017;33:65–69.
  21. Lallas A, Kyrgidis A, Tzellos TG, Apalla Z, Karakyrriou E, Karatolias A, *et al.* Accuracy of dermoscopic criteria for the diagnosis of psoriasis, dermatitis, lichen planus and pityriasis rosea. *Br J Dermatol* 2012;166:1198–1205. doi: 10.1111/j.1365-2133.2012.10868.x.
  22. Fujisawa Y, Otomo Y, Ogata Y, Nakamura Y, Fujita R, Ishitsuka Y, *et al.* Deep learning-based, computer-aided classifier developed with a small dataset of clinical images surpasses board-certified dermatologists in skin tumor diagnosis. *Br J Dermatol* 2018;179:373–381. doi: 10.1111/bjd.16924.
  23. Panchal G, Ganatra A, Kosta YP, Panchal D. Behaviour analysis of multilayer perceptrons with multiple hidden neurons and hidden layers. *Int J Comput Theory Eng* 2011;3:332–337. doi: 10.7763/IJCTE.2011.V3.328.
  24. Esteva A, Kuprel B, Novoa RA, Ko J, Swetter SM, Blau HM, *et al.* Dermatologist-level classification of skin cancer with deep neural networks. *Nature* 2017;542:115–118. doi: 10.1038/nature21056.
  25. Shin HC, Roth HR, Gao M, Lu L, Xu Z, Nogues I, *et al.* Deep convolutional neural networks for computer-aided detection: CNN architectures, dataset characteristics and transfer learning. *IEEE Trans Med Imaging* 2016;35:1285–1298. doi: 10.1109/tmi.2016.2528162.
  26. Szegedy C, Vanhoucke V, Ioffe S, Shlens J, Wojna Z. Rethinking the Inception Architecture for Computer Vision. *IEEE Conference on Computer Vision and Pattern Recognition*. Las Vegas, USA; 2016. p. 2818–2826.
  27. Haenssle HA, Fink C, Schneiderbauer R, Toberer F, Buhl T, Blum A, *et al.* Man against machine: diagnostic performance of a deep learning convolutional neural network for dermoscopic melanoma recognition in comparison to 58 dermatologists. *Ann Oncol* 2018;29:1836–1842. doi: 10.1093/annonc/mdy166.
  28. Zhang X, Wang S, Liu J, Tao C. Towards improving diagnosis of skin diseases by combining deep neural network and human knowledge. *BMC Med Inform Decis Mak* 2018;18 (Suppl 2):59. doi: 10.1186/s12911-018-0631-9.
  29. Han SS, Kim MS, Lim W, Park GH, Park I, Chang SE. Classification of the clinical images for benign and malignant cutaneous tumors using a deep learning algorithm. *J Invest Dermatol* 2018;138:1529–1538. doi: 10.1016/j.jid.2018.01.028.
  30. Tschandl P, Argenziano G, Razzmaria M, Yap J. Diagnostic accuracy of content-based dermatoscopic image retrieval with deep classification features. *Br J Dermatol* 2018;181:155–165. doi: 10.1111/bjd.17189.
  31. Brinker TJ, Hekler A, Utikal JS, Grabe N, Schandorf D, Klode J, *et al.* Skin cancer classification using convolutional neural networks: systematic review. *J Med Internet Res* 2018;20:e11936. doi: 10.2196/11936.
  32. Navarrete-Dechent C, Dusza SW, Liopyris K, Marghoob AA, Halpern AC, Marchetti MA. Automated dermatological diagnosis: hype or reality? *J Invest Dermatol* 2018;138:2277–2279. doi: 10.1016/j.jid.2018.04.040.
  33. Maron RC, Weichenthal M, Utikal JS, Hekler A, Berking C, Hauschild A, *et al.* Systematic outperformance of 112 dermatologists in multiclass skin cancer image classification by convolutional neural networks. *Eur J Cancer* 2019;119:57–65. doi: 10.1016/j.jaad.2017.08.016.
  34. Hekler A, Utikal JS, Enk AH, Hauschild A, Weichenthal M, Maron RC, *et al.* Superior skin cancer classification by the combination of human and artificial intelligence. *Eur J Cancer* 2019;120:114–121. doi: 10.1016/j.ejca.2019.07.019.
  35. Brinker TJ, Hekler A, Enk AH, Berking C, Haferkamp S, Hauschild A, *et al.* Deep neural networks are superior to dermatologists in melanoma image classification. *Eur J Cancer* 2019;119:11–17. doi: 10.1016/j.ejca.2019.05.023.
  36. Brinker TJ, Hekler A, Enk AH, Klode J, Hauschild A, Berking C, *et al.* Deep learning outperformed 136 of 157 dermatologists in a head-to-head dermoscopic melanoma image classification task. *Eur J Cancer* 2019;113:47–54. doi: 10.1016/j.ejca.2019.04.001.
  37. Brinker TJ, Hekler A, Enk AH, Klode J, Hauschild A, Berking C, *et al.* A convolutional neural network trained with dermoscopic images performed on par with 145 dermatologists in a clinical melanoma image classification task. *Eur J Cancer* 2019;111:148–154. doi: 10.1016/j.ejca.2019.02.005.
  38. Jun G, Shukui Q, Jun L, Tongyu L, Lu S, Xiaohong C, *et al.* Chinese guidelines on the diagnosis and treatment of melanoma (2015 edition) (in Chinese). *Chin Clin Oncol* 2016;5:57. doi: 10.21037/cco.2015.12.02.
  39. Marchetti MA, Codella NCF, Dusza SW, Gutman DA, Helba B, Kalloo A, *et al.* Results of the 2016 international skin imaging collaboration international symposium on biomedical imaging challenge: comparison of the accuracy of computer algorithms to dermatologists for the diagnosis of melanoma from dermoscopic images. *J Am Acad Dermatol* 2018;78:270–277. doi: 10.1016/j.jaad.2017.08.016.
  40. Wang S, Liu J, Zhu C, Shu C, Zhou H, Xie F, *et al.* Comparison of diagnostic performance of dermatologists versus deep convolutional neural network for dermoscopic images of pigmented nevus and seborrheic keratosis (in Chinese). *Chin J Dermatol* 2018;51:486–489. doi: 10.3760/cma.j.issn.0412-4030.2018.07.002.
  41. Ding X, Wang T, Shen Y, Wang X, Zhou C, Tian S, *et al.* Prevalence of psoriasis in China: a population-based study in six cities. *Eur J Dermatol* 2012;22:663–667. doi: 10.1684/ejd.2012.1802.
  42. Li CX, Shen CB, Xue K, Shen X, Jing Y, Wang ZY, *et al.* Artificial intelligence in dermatology: past, present, and future. *Chin Med J* 2019;132:2017–2020. doi: 10.1097/CM9.0000000000000372.
- 
- How to cite this article:** Wang SQ, Zhang XY, Liu J, Tao C, Zhu CY, Shu C, Xu T, Jin HZ. Deep learning-based, computer-aided classifier developed with dermoscopic images shows comparable performance to 164 dermatologists in cutaneous disease diagnosis in the Chinese population. *Chin Med J* 2020;133:2027–2036. doi: 10.1097/CM9.0000000000001023